



HAL
open science

REVIEW OF RECENT EXPERIMENTAL RESULTS FROM THE STANFORD $3\mu\text{m}$ FREE ELECTRON LASER

S. Benson, D. Deacon, J. Eckstein, J. Madey, K. Robinson, T. Smith, R. Taber

► **To cite this version:**

S. Benson, D. Deacon, J. Eckstein, J. Madey, K. Robinson, et al.. REVIEW OF RECENT EXPERIMENTAL RESULTS FROM THE STANFORD $3\mu\text{m}$ FREE ELECTRON LASER. Journal de Physique Colloques, 1983, 44 (C1), pp.C1-353-C1-362. 10.1051/jphyscol:1983128 . jpa-00222557

HAL Id: jpa-00222557

<https://hal.science/jpa-00222557>

Submitted on 4 Feb 2008

HAL is a multi-disciplinary open access archive for the deposit and dissemination of scientific research documents, whether they are published or not. The documents may come from teaching and research institutions in France or abroad, or from public or private research centers.

L'archive ouverte pluridisciplinaire **HAL**, est destinée au dépôt et à la diffusion de documents scientifiques de niveau recherche, publiés ou non, émanant des établissements d'enseignement et de recherche français ou étrangers, des laboratoires publics ou privés.

REVIEW OF RECENT EXPERIMENTAL RESULTS FROM THE STANFORD 3 μ m FREE ELECTRON LASER*

S. Benson, D.A.G. Deacon⁺, J.N. Eckstein⁺⁺, J.M.J. Madey, K. Robinson,
T.I. Smith and R. Taber⁺⁺⁺

*High Energy Physics Laboratory, Stanford University, Stanford,
California 94305, U.S.A.*

Résumé - De nouvelles mesures ont été faites sur le Laser à Electrons Libres de Stanford en utilisant un faisceau d'électrons de meilleure qualité. Pour la première fois, nous avons étudié la structure temporelle des impulsions optiques en employant une technique d'autocorrélation optique. Les nouvelles mesures sont comparées avec les mesures précédentes. Certains aspects énigmatiques des mesures précédentes semblent être corrélés avec les caractéristiques du faisceau d'électrons. Les résultats d'expériences d'autocorrélation indiquent que la longueur des impulsions optiques est voisine de celle donnée par la simple transformée de Fourier du spectre. Les impulsions sont plus courtes que prévues lorsque la longueur de la cavité est plus courte que la longueur de synchronisme. Nous relatons aussi des expériences faites sur le deuxième harmonique et sur les effets du champ magnétique solénoïdal sur le fonctionnement du laser.

Abstract - New data has been taken on the Stanford Free Electron Laser (FEL) with improved electron beam characteristics. For the first time we have studied the temporal structure of the optical pulses using optical autocorrelation techniques. The new data is compared and contrasted with earlier data. Several puzzling aspects of the previous data appear correlated with drifts in the spectrum and current of the electron beam. Autocorrelation results indicate nearly transform limited pulses which are shorter than expected at large values of the cavity length detuning. We also report here experiments carried out to study the intrinsic second harmonic radiation and the effects of the superimposed solenoidal magnetic field on laser operation.

1.- INTRODUCTION

In March of 1981, the Stanford Free Electron Laser was operated with comprehensive diagnostics for the first time allowing us to study the time dependence of the optical and electron beam properties. The results of these experiments were not only inconsistent with those of numerical simulations but also displayed very puzzling behavior which was impossible to explain by any simple model. These included anomalously long turn-on times and extended development of the optical and electron beam spectra during the full millisecond the laser was on.[1]. In an effort to explain these strange effects and to shed some light on the lack of agreement between theory and experiment, the laser was operated again in August of the same year. In addition,

*Work supported in part by the Office of Naval Research under contract N00014-78-C-0403

⁺Presently at Deacon Research, 3790 El Camino Real, Palo Alto, CA 94306, U.S.A.

⁺⁺

Presently at Varian Associates, Palo Alto, California, U.S.A.

⁺⁺⁺

Presently at GenRad Inc., Cupertino, California, U.S.A.

an apparatus was installed to measure the time dependent autocorrelation function of the optical pulses. This provided the first evidence of the time domain structure of the optical pulses [2]. In this paper we compare the results of the March and August runs, and review the new measurements of the autocorrelation functions, the harmonic spectrums, and the effects of the solenoidal field.

Both theoretical models of sideband instabilities and numerical simulations predict an autocorrelation function with strong intensity modulation [3]. Despite adequate resolution, we could detect no such substructure on the pulse. In addition, the time bandwidth product indicates that the pulses are nearly Fourier transform limited. This fact, coupled with the simple form of the optical spectra, indicates that pulses are structureless and have very little frequency variation within the pulse (chirp).

Largely due to differences in the characteristics of the electron beam, the data obtained in August differed quite remarkably from the data taken in March. These differences have led us to a possible explanation for some of the more puzzling aspects of the earlier data. The anomalous turn-on times and extended evolution of the optical and electron momentum spectra appear correlated with small drift in the spectra and current of the electron beam. The sensitivity of these parameters to the electron beam qualities is, in itself, an intriguing result.

In addition to these observations, we report the results of two new experiments to study the effect of the superimposed solenoidal field and the characteristics of the intrinsic second harmonic radiation generated in the laser.

2. - EXPERIMENTAL SETUP

The laser configuration in the August run was similar to that of previous runs. The electron beam was provided by the Stanford Superconducting Accelerator (SCA) which was operated at 43 MeV and provided 5.6 pC bunches of length 2.5 psec (FWHM) separated by 84.6 nsec intervals. The peak current density was $2 \times 10^{11} \text{ cm}^{-3}$. This energy provides laser operation at 3.2 μm . The cavity consists of two dielectric quarter wave stack mirrors with 7.5 m radii of curvature separated by 12.68 m. Cavity losses were measured at 1.5% per pass. The ratio of power radiated by the electron beam to that emerging at the output coupler was 3 to 1. On the basis of the measured optical pulse length, the instantaneous peak optical power radiated by the electron beam was 400 kW. The optical and electron momentum spectra were measured using standard apparatus described elsewhere [1,4]. The optical power measurements were carried out by relaying the laser beam through a 50 meter optical transport system into the apparatus shown in figure 1. The autocorrelation function, the optical power, and the second harmonic generated in a nonlinear crystal could be measured using this setup. The autocorrelation apparatus is a standard Michelson interferometer used in conjunction with a lithium niobate second harmonic generation crystal [5]. The generated second harmonic power is given by,

$$P_{sh} = 2 \eta \int I(t)^2 dt + 4 \eta \int I(t) I(t+\tau) dt$$

where η is the conversion efficiency, τ is the time lag between the two pulses in the interferometer, and $I(t)$ is the intensity vs. time of each of the two pulses. This expression has been averaged over the fine scale fringe structure present in any interferometer. As one mirror is moved the second harmonic power will change from the baseline value due to the two separate pulses to a peak which is a factor of three higher, thereby defining the autocorrelation function. The fundamental power was blocked from entering the Ge:Au detectors by a pair of bandpass optical filters. These provided a rejection ratio of 10^6 to 1 for the fundamental. Time dependent autocorrelation records were taken by sampling the detector at 128 sequential points in time on successive beam pulses. Thirty-two measurements were recorded and averaged at each position of the moving mirror. This large number of samples was needed to average out the fringe structure as noted below. Time averaged records were computed by summing all data taken at a given mirror position.

The time dependence of the generated second harmonic could be measured by blocking the moving arm of the interferometer, typically sampling the detector 1024 times each macropulse and averaging over up to 128 pulses. When measuring the power at the fundamental, the lithium niobate crystal was detuned and the bandpass filters were replaced with a low-pass black glass filter.

As noted above, measurement of the autocorrelation function requires averaging over the fine scale fringe structure present due to the nature of the interferometer. This averaging was accomplished by shaking the mirror stage with a PZT pusher driven by a Gaussian noise source. The major source of noise in the autocorrelation measurement was these fringes. The noise was reduced by averaging over many beam pulses,

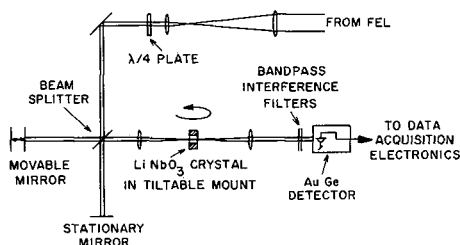


Figure 1. - Optical autorrelation apparatus. The laser light's polarization is changed from circular to horizontal using the quarter wave plate. It is then split in a Michelson interferometer and recombined in a LiNbO_3 frequency doubling crystal. Bandpass filters block out laser light at the fundamental.

but time constraints limited the amount of averaging possible. One also needs perfect lateral overlap of the two pulses at the focus of the lens to get the expected 3 to 1 ratio of signal to background. We only achieved a ratio of 2.5 to 1, indicating a slight misalignment of the optics.

The longitudinal charge distribution of the individual bunches was measured by placing an rf cavity in the beam line with the field transverse to the beam, and adjusting the phase of the field so that electrons at the center of the bunch were undeflected. The angular distribution of the electrons emerging from the cavity can be expressed as a convolution of the electrons longitudinal and transverse distribution. The actual longitudinal charge distribution can be constructed by analyzing the angular distributions taken with the cavity turned on and off.

The initial part of the SCA electron beam pulse contains relatively large fluctuations in the beam position, bunch length, and energy. In the previous run, this unstable part of the beam was deflected out of the system using the transverse deflection cavity. The cavity was turned off after the initial sections of the accelerator had come into regulation. This reduced the current and energy fluctuations substantially but did not eliminate them all-together since the final sections of the accelerator still suffered transient beam loading. The initial turn-on transients were eliminated completely in the August run by placing a set of electrostatic deflection plates after the last accelerator section. The plates were used to deflect the electrons out of the beamline until the accelerator came into regulation. The resulting current and energy waveforms were very nearly ideal step functions with negligible drift following turn-on. Figure 2 shows the time development of the electron momentum with the deflection cavity and with the electrostatic deflection plates. The rise time for the beam current to reach 90% of full current was measured to be 6 μsec .

3. - RESULTS

Turn-on-Time: The turn-on-time observed in August using the two new deflection plates differed substantially from those seen in the March run. The new data, including the 1/e rise time; gain, and the delay time needed to reach 50% of the final power, are listed in table 1 as a function of the cavity length detuning δL .

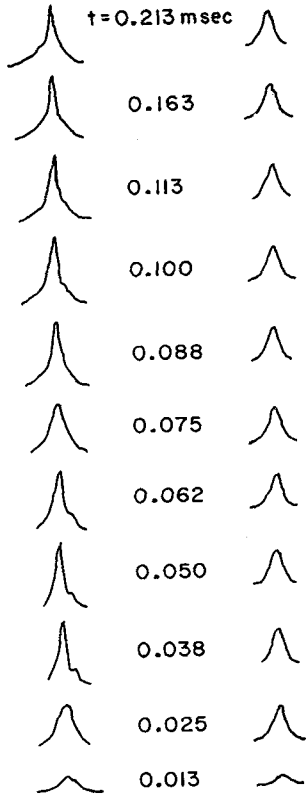


Fig. 2. - Electron momentum spectra as a function of time during accelerator pulse. The set of curves on the left was taken using a transverse deflection cavity after the first accelerator section. The set on the right was taken using a pair of deflection plates at the exit of the accelerator. The momentum range for each scan is 0.5%.

This parameter is defined as the change in the optical round-trip length in the laser cavity as the output mirror is moved. It is reported in thousandths of an inch and is measured with respect to the peak in the power vs. cavity length detuning curve.

As in the previous data, maximum gain occurs at $\delta L = -0.3$. But in contrast to the earlier data, the turn-on times are quite reasonable. The ratio of the delay time to the $1/e$ rise time is less than 30 in all cases. This ratio was as large as 60 in the March data.

Time-Dependent Frequency Shifts: One other curious feature present in the March data is the long term drift of the optical wavelength. This was not seen in the data taken in August. Figure 3 shows time dependent records of the optical spectra taken at $\delta L = 0$ for the two runs. The new data is essentially time independent. In an effort to determine the source of this discrepancy, we reviewed the March data taken on the time-dependent optical spectra and the zeroth, first, and second moments of the electron momentum distribution. In the initial part of the pulse the wavelength shift was almost directly proportional to the first moment of the energy distribution. Such a case is shown in figure 4. The ratio of the change in wavelength to mean energy is two, matching the change in the resonant wavelength. Later in the pulses however, the laser wavelength shifted while the electron energy remained constant. In these cases the shift appears correlated with changes in the zeroth and second moments (beam current and energy spread) of the electron momentum spectrum. In the August data, all three moments of the electron spectrum were essentially constant and no wavelength shift was seen.

Table 1

Gain and Rise Times for Different Cavity Lengths

Cavity Length detuning	1/e rise time	Gain Per Pass*	Delay Time
$\delta L = 0.0 \times 10^{-3}$	1.72 μ sec	6.5%	46 μ sec
$= -0.3 \times 10^{-3}$	1.06 μ sec	9.8%	31 μ sec
$= -0.5 \times 10^{-3}$	1.22 μ sec	8.7%	33 μ sec

* This is the net gain added to the loss of the cavity and represents the actual gain of the electron beam. It is measured at approximately 1/100 of the final power.

Note that the correlation of mean frequency and energy spread observed in March implies a high sensitivity to energy spread. In one case, a change in the width of the electron beam spectrum, from 0.03% to 0.035% produced a 0.15% change in the optical wavelength.

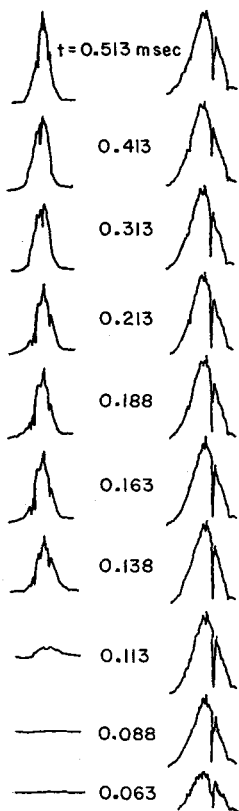


Figure 3.- Optical spectra as a function of time for the March run (left) and the August run (right). Note the frequency shifts present in the March data. The wavelength range for each scan is 29 nm.

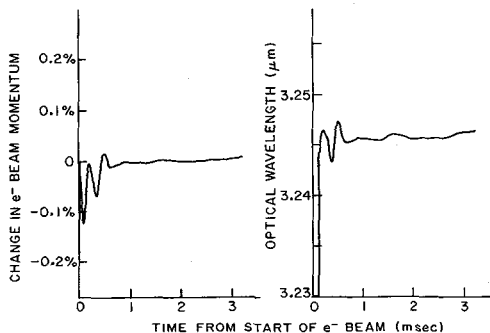
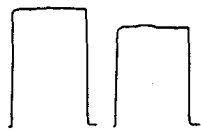


Figure 4.- First moments of the (a) electron moment and (b) optical spectra for data taken in March without the initial transient knocked out of the beam. One expects the relative shift in the wavelength to be twice that of the electron momentum.

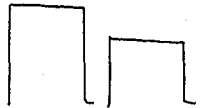
Time-Dependent Optical Pulse Shape: As noted above, the mean optical wavelength in the August experiments remained essentially constant after the initial laser turn-on. Unfortunately, the signal-to-noise ratio in the autocorrelation records was not good enough to show that this was also true in the time domain. It was possible, however, to look at the evolution of the ratio of the generated second harmonic power to the fundamental power squared. This ratio should be inversely proportional to the optical pulse length. The optical power and generated second harmonic power for $\delta L = 0.0, -0.3, -0.5,$ and 0.7 are plotted in figure 5. The ratio P_{sh} / P_{fund}^2 for these

records is constant to a few percent after the initial turn-on. It is also interesting to note that the laser power is increasingly sensitive to electron beam variations as the cavity is shortened. This is similar to the sensitivity to perturbations that any laser experiences near threshold.

Autocorrelation Function: Since the August data was essentially time independent after the initial turn-on, we averaged the optical spectra and autocorrelation records over the length of the beam pulses. The time averaged autocorrelation function



(a) STABLE MAXIMUM



(b) $\delta L = -0.3$



(c) $\delta L = -0.5$



(d) $\delta L = -0.7$

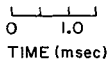


Figure 5.- The time dependence of the optical power (left) and the second harmonic power generated in a LiNbO_3 crystal (right). For constant optical pulse width, one expects the second harmonic to be proportional to the square of the first.

Figure 7.- Time averaged optical spectra as function of cavity length detuning. The dip present in all curves is believed to be due to intracavity absorption.

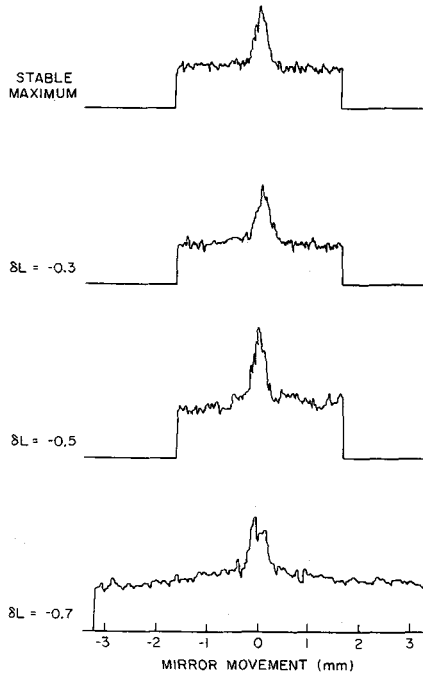
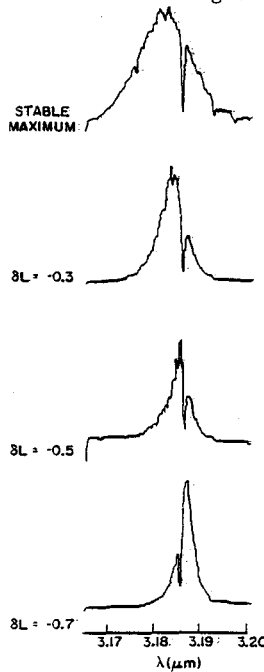


Figure 6.- Time averaged autocorrelation data as a function of the cavity length detuning. The base-line is included to indicate the signal to back-ground ratio of 2.5 to 1. Note the long tail at $\delta L = -0.7$.



for the four detunings noted above are shown in figure 6. The pulse lengthens as the cavity is shortened from its stable maximum at $\delta L = 0.0$ and develop a long tail at $\delta L = -0.7$. No statistically significant substructure is seen in any of the records. Figure 7 shows the optical spectra for the same cavity lengths. The dips in each spectrum are due to intracavity absorption by gasses desorbed from the bore by the electron beam. As the cavity is lengthened, the spectra become narrower as expected from the inverse nature of the time and frequency domains. Note that the change in spectral width by a factor of two between $\delta L = 0$ and $\delta L = -0.3$ is only accompanied by a 20% change in the pulse length. There are several possible reasons for this. The simplest of these is that there is a significant amount of frequency variation correlated with position in the pulse (chirp). The FWHM widths of the spectra and autocorrelation records is listed in Table 2. The autocorrelation width expected assuming a Gaussian and a Lorentzian line shape and Fourier transform limited time-bandwidth product are also listed.* The measured widths are close to or between the two limits in all cases, indicating near transform limited pulses.

One expects a single sided exponential pulse shape at large negative detunings and the data is consistent with this shape, but the actual length is not what one would expect from a simple model. When the cavity length is shorter than the synchronous length the optical pulse is pushed ahead of the electron pulse and so should develop a long tail in the forward direction. If one assumes that the leading tail experiences no interaction then it will decay with a life-time characteristic of the cavity decay time and so one expects the tail to be exponential. It is simple to calculate the length expected from this model and the values obtained agree well with those obtained in numerical simulations. They are larger by a factor of three than those seen, however. This seems to indicate a more complicated behavior than one would expect from naive considerations.

Table 2

Spectral and Autocorrelation Function Widths

δL (0.001")	$\Delta\tau$ (psec)	$\Delta\nu$ (10^{12})	$\Delta\tau_G$ (psec)	$\Delta\tau_L$ (psec)
0	1.5 ± 0.3	0.36 ± 0.02	1.7	0.61
-0.3	1.8 ± 0.3	0.16 ± 0.01	3.9	1.4
-0.5	1.8 ± 0.3	0.11 ± 0.01	5.7	2.0
-0.7	2.7 ± 0.3	0.10 ± 0.01	6.2	2.2

Electron Bunch Shape: As noted in section 2, the electron bunch length can be found by analyzing the cavity-on and cavity-off records from the transverse deflection cavity. In practice this was done by assuming Gaussian longitudinal and transverse distributions, and fitting their parameters to the observed angular distributions. The results of this calculation are shown in figure 8. The bunch length of the best fit is 2.5 psec. This is shorter than that of the previous run.

Associated with this change in bunch lengths, the electron momentum spectra in the two runs were substantially different. The electron momentum spectra with the laser on and operating at the stable maximum in the detuning curve is shown in figure 9 for the two runs. The spectrum for the August run actually resembles the distribution function for a simple harmonic oscillator. A possible interpretation of this result is that, at 2.5 psec, the electron bunch is short enough to insure that all the electrons in the bunch see essentially the same optical field.

* The transform-limited product for the autocorrelation function and the optical spectrum depends on the form used for each. If both are Gaussian, the product is $4\sqrt{2}\ln 2$. If the optical pulse shape is a single-sided exponential, and the spectrum is a Lorentzian, the product is $2\ln 2$. Note that the FWHM time-bandwidth product is not a minimum for Gaussian pulses.

Harmonics: Unlike most lasers the FEL emits radiation at harmonic frequencies of the laser radiation. Harmonics were not expected to be seen in a helical wiggler though. Nevertheless, we detected optical power at the second harmonic which was a factor of 10^{-4} of the power at the fundamental. No power was detected at the third harmonic, though our sensitivity was not good enough to detect power at $1 \mu\text{m}$ at 10^8 below the fundamental power. The second harmonic radiation has an angular extent and spectral characteristics similar to the fundamental. The polarization was tested using a Brewster plate and the radiation was found not to be longitudinally polarized. The ratio of the relative spectral widths of the fundamental and the second harmonic was 0.8.

There are many ways to produce second harmonic radiation in an FEL but most do not produce as much power as was seen. Non-linear conversion in the mirrors and windows could not contribute more than a fraction of 10^{-8} of the fundamental. Any radiation produced in the dipole bending magnets would be linearly polarized. The distortion of the helical orbits by the off-axis field gradients could contribute at most 10^{-7} . We now believe that off-axis radiation is responsible for the second harmonic. The ratio of second harmonic power to fundamental power varies as the square of the angle between the direction of observation and the average velocity of the electron [6]. Calculations on a zero emittance perfectly bunched beam of finite radial extent ($300 \mu\text{m}$ waist) indicate a harmonic production of 0.0026 times the fundamental. Actual bunching will produce less than this since the bunching present at the fundamental is not as effective in producing coherent second harmonic radiation.

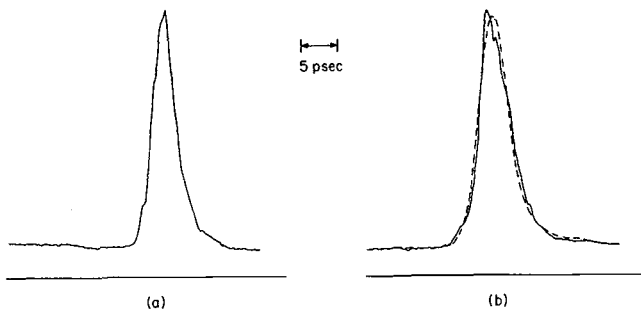


Figure 8.- The electron density profiles recorded with a pick-off wire with bunch length measuring cavity off (a) and on (b). The dashed curve is the convolution of a 2.5 psec long gaussian longitudinal profile with the cavity-off curve.

Solenoid Field: The magnetic field in the wiggler consists of a helical field with a superimposed solenoid field. We varied the solenoid current, normally at 100 A, from 90 A to 120 A. The laser output power remained essentially constant, though the steering had to be readjusted at each current. The time averaged electron momentum spectrum and optical spectrum were also recorded at each current. The optical spectra appear to be similar at all currents, but the electron momenta differ somewhat. The electron momentum spectra for solenoid currents of 90 A (a) and 120 A (b) are shown in figure 10. The two curves are shifted with respect to each other by 0.25% to indicate the scale. The difference is noticeable and probably deserves study.

4.- SUMMARY

The new data from the FEL has resolved several perplexing questions. The anomalously large turn-on times disappear when the turn-on transients of the electron beam are

eliminated, and the time-dependent wavelength shifts are eliminated with a stable electron momenta spectrum. We have also discovered a reasonable mechanism for the observed second harmonic radiation.

But the data also raises some new questions. Assuming the observed correlation of optical wavelengths, currents, and energy spread indicates a causal relationship, why is the wavelength so sensitive to the spread and current? Why are the sub-pulses predicted by theory not present in the optical autocorrelation function? And why are the optical pulses at large detuning so short? While much progress has been made, significant further effort will be required to resolve these questions.

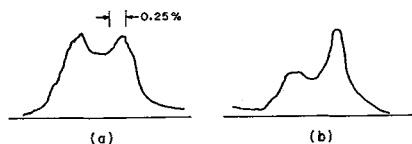


Figure 9.- Electron momentum spectra taken with the laser on and operating at the stable maximum in the cavity length detuning curve, (a) August data and (b) March data.

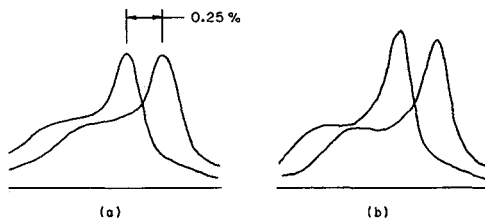


Figure 10. - Time averaged electron momentum spectra taken when the solenoid current was set at 90 A (a) and 120 A (b). Two curves were taken with a 0.25% energy offset to get the energy calibration.

5.- ACKNOWLEDGEMENT

It is a pleasure to acknowledge the assistance of Sam Brain, Marcel Marc, Michael McAshan, Roy Rand, Renato Redaelli and the staff of the High Energy Physics Laboratory.

6.- BIBLIOGRAPHY

- [1]. ECKSTEIN, J. N., MADEY, J. M. J., ROBINSON, K., SMITH, T. I., BENSON, S., DEACON, D., TABER, R. and GAUPP, A., in Physics of Quantum Electronics, Vol. 8, p. 49, edited by JACOBS, S. K. et al. (Addison-Wesley, Reading, Mass., 1982).

- [2]. BENSON, S., DEACON, D.A.G., ECKSTEIN, J. N., MADEY, J. M. J., ROBINSON, K., SMITH, T. I., and TABER, R., *Phys. Rev. Lett.* 48, 235 (1982).
- [3]. COLSON, W. B., in Physics of Quantum Electronics, Vol. 8, p. 457, edited by JACOBS, S. K., et al. (Addison-Wesley, Reading, Mass., 1982).
- [4]. DEACON, D.A.G., ELIAS, L. R., MADEY, J. M. J., RAMIAN, G. J., SCHWETTMAN, H.A., SMITH, T. I., *Phys. Rev. Lett.* 38, 892 (1977).
- [5]. IPPEN, E. P., and SHANK, C. V., in Topics in Applied Physics, edited by SHAPIRO, S. L. (Springer-Verlag, Berlin 1977). Vol. 18, p. 83.
- [6]. COLSON, W. B., Ph.D. Dissertation, (Stanford University, unpublished) 1977.